# Methylglyoxal induced glycation and aggregation of human serum albumin: Biochemical and biophysical approach

Azaj Ahmed [a], Anas Shamsi [a], Mohd Shahnawaz Khan [b], Fohad Mabood Husain [c], Bilqees Bano [a,*]

[a] Department of Biochemistry, F/O Life Sciences, Aligarh Muslim University, Aligarh, India
[b] Protein Research Chair, Department of Biochemistry, College of Sciences, King Saud University, Riyadh, Saudi Arabia
[c] Department of Food Science and Nutrition, Faculty of Food and Agricultural Sciences, King Saud University, 2460, Riyadh 11451, Saudi Arabia

## ARTICLE INFO

## ABSTRACT

Serum protein glycation and formation of advanced glycation end products (AGEs) correlates with many diseases viz. diabetes signifying the importance of studying the glycation pattern of serum proteins. In our present study, methylglyoxal was investigated for its effect on the structure of human serum albumin (HSA); exploring the formation of AGEs and aggregates of HSA. The analytical tools employed includes intrinsic and extrinsic fluorescence, UV spectroscopy, far UV circular dichroism, Thioflavin T fluorescence, congo red binding, polyacrylamide gel electrophoresis (PAGE). UV and fluorescence spectroscopy revealed the structural transition of native HSA evident by new peaks and increased absorbance in UV spectra and quenched fluorescence in the presence of MG. Far UV CD spectroscopy revealed MG induced secondary structural alteration evident by reduced α-helical content. AGEs formation was confirmed by AGEs specific fluorescence. Increased ThT fluorescence and CR absorbance of 10 mM MG incubated HSA suggests that glycated HSA results in the formation of aggregates of HSA. SEM and TEM were reported to have an insight of these aggregates. Molecular docking was also utilized to see site specific interaction of MG-HSA. This study is clinically significant as HSA is a clinically relevant protein which plays a crucial role in many diseases.

© 2018 Elsevier B.V. All rights reserved.

## 1. Introduction

Proteins synthesized on ribosome undergo post translational modifications in a bid to attain a unique three-dimensional structure to fulfil their physiological functions. Anomalies in modification process leads to formation of misfolded proteins, these misfolded proteins either detected by protein quality control system and gets degraded or may left unnoticed and forms toxic aggregates. This misfolding of proteins is at heart of many disorders. The accumulated toxic aggregates of proteins cause myriad of diseases ranging from neurodegenerative disorders such as Alzheimer's, Parkinson's diseases to diabetes mellitus and hence drew the attention of scientific community owing to their clinical importance. One feature of protein is glycation where sugars have damaging effect on structural and non-structural proteins thereby distorting native structure of a protein. Glycation is a non-enzymatic process that involves multiple parallel and consecutive reactions often collectively called the Maillard reaction. The key steps includes the formation of Schiff base, followed by Amadori rearrangement and advanced glycation end products (AGEs) formation are the key steps of protein glycation [1].

The model protein used for our present study is human serum albumin (HSA). The prominence of HSA arises from the statement that it is the most abundant protein in human blood plasma prone to glycation [2]. HSA is a monomeric globular protein consisting of 585 amino acid residues with corresponding molecular mass of 66.446 kDa. Amino acids residues of HSA prone to glycation are: N-terminal Asp, 59 Lys, 24 Arg, and one free cysteinyl thiol (17 disulfide bonds) [3]. HSA plays many different roles viz. responsible for maintaining osmotic pressure in the circulatory system [4] and may also play a protective role in vivo as an antioxidant [5].

There are various compounds that can denature proteins and forms aggregates in solution thereby mimicking in vivo environment. Organic solvents destroy the hydrophobic interactions thereby altering the native tertiary structure of the proteins [6]. In a bid to cause unfolding of the ordered secondary structure of the polypeptide chain, very high concentrations of these solvents are required [7,8]. One such solvent is methylglyoxal (MG). MG is an extremely reactive aldehyde or dicarbonyl, contributing in majority of diseases such as diabetic vascular complications, atherosclerosis, cataracts and many more [9]. The importance of MG comes from the view that it is reported in many studies that MG acts by modifying protein to its toxic aggregates. Protein aggregates
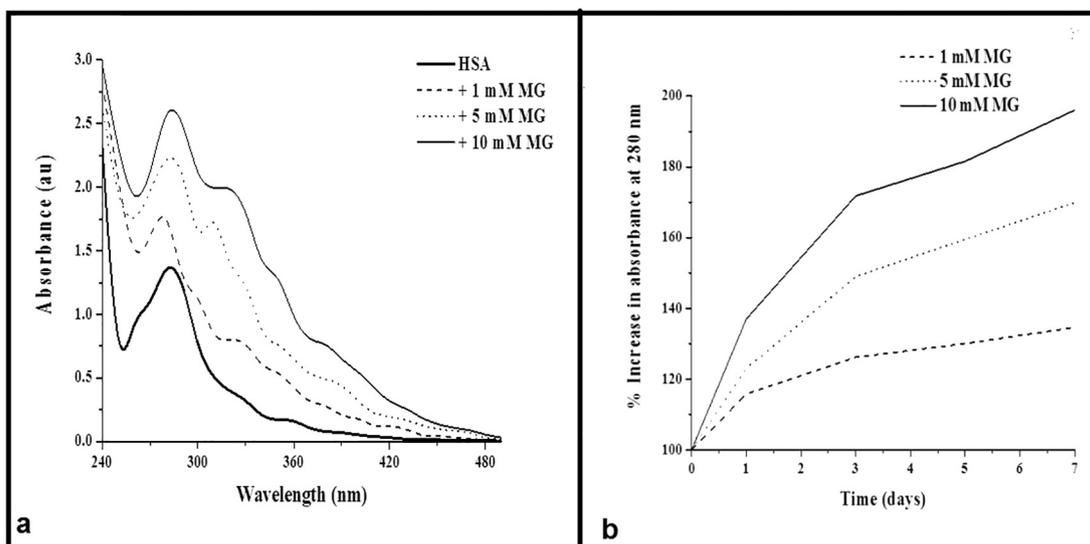
**Fig. 1.** (a) Ultraviolet spectrum of native and HSA incubated with varying concentration of MG (1, 5 and 10 mM). The spectra were recorded in wavelength range of 240 nm–480 nm. Cells of 1 cm path length were used. (b) Percent change in absorbance at 280 nm upon incubating HSA with MG.

such as amyloid plaques, intracytoplasmic or intranuclear inclusions and neurofibrillary tangles are believed to cause imbalance in ion homeostasis, damage to cell membrane, stimulation of apoptosis and cell death [10]. Thus, it is imperative to study detailed mechanism of glycation induced changes in the protein's conformation making it liable to amyloid aggregation.

Alzheimer's, Parkinson's and familial amyloid polyneuropathy in a way or other are associated with protein misfolding and aggregation [11]. Many studies have reported association of HSA in various disorders [12] thus increasing the interest of researchers to work on this clinically relevant protein. Protein aggregation into oligomers and fibrils are associated with many human pathophysiology's [13]. In pathogenesis of various neurodegenerative disorders amyloid fibrils are at the heart [14]. In light of reported literature which highlights the clinical importance of HSA and MG, the present work was undertaken. The present work was aimed at analysing the changes in structure of HSA in the presence of MG. In our study, insight into aggregation and glycation pattern of HSA induced by MG is undertaken. Our study tries to have an insight into the aggregation and glycation pattern of HSA with varying MG concentrations so as to be aware of how HSA aggregates and glycates in the presence of MG.

## 2. Materials

Human serum albumin was purchased from Sigma (St. Louis, MO, US). 8-Anilino-1-Naphthalene-Sulphonic acid (ANS), Thioflavin T (ThT) and Congo red (CR) were bought from Sigma (St. Louis, MO, USA).

## 3. Methods

### 3.1. Glycation of HSA

50 μM HSA was incubated in sodium phosphate buffer, 1 mM $NaN_3$, in the presence of methyl glyoxal (1, 5 and 10 mM) for 7 days at 37 °C. Pure native HSA was incubated under the same conditions and was used as a control. After the incubation, HSA-MG and control HSA were extensively dialyzed against sodium phosphate buffer at 4 °C. Protein concentrations were determined by the method of Lowry et al. 1951 [15].
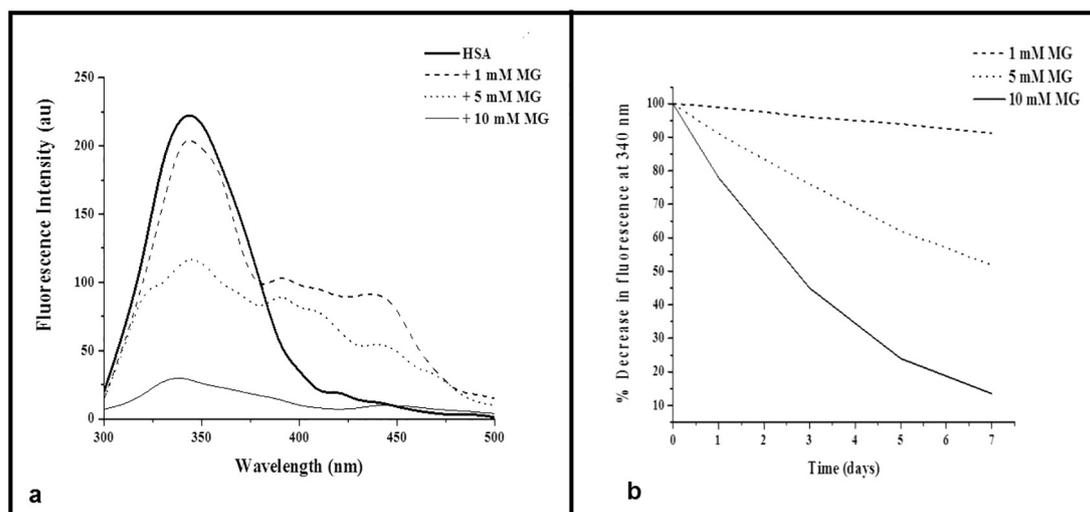


**Fig. 2.** (a) Intrinsic fluorescence spectra of native HSA and HSA incubated with varying MG concentration (1, 5 and 10 mM). The excitation wavelength was 280 nm while spectra were recorded in the range of 300–400 nm. (b) Percent change in fluorescence at 340 nm upon incubating HSA with MG. Aliquots were withdrawn at regular time intervals for spectral analysis. Percent change in fluorescence was calculated taking the value of sample incubated without sugars as control.
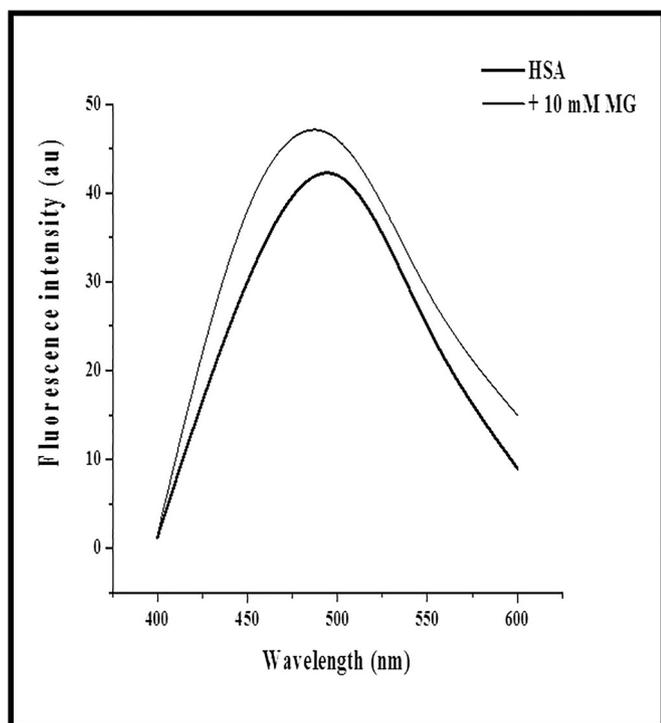
**Fig. 3.** Fluorescence spectra of ANS binding at excitation wavelength 385 nm: native HSA and HSA incubated with 10 mM MG. Spectra were taken at the end of incubation period.

### 3.2. Molecular docking analysis

Molecular docking was carried out to decode the sites of interaction between HSA and methylglyoxal using well-established docking software AutoDockVina [16]. The three dimensional crystal structure of HSA was downloaded from RCSB Protein Data Bank [PDB: 1AO6]. All the water molecules were removed in a bid to avoid any hindrance. The 3D structure of methylglyoxal was downloaded from https://pubchem.ncbi.nlm.nih.gov in SDF format which was converted to pdb format using Chimera 1.10.2. All additional docking factors were kept as default and Accelrys Discovery Studio 4.5 was employed for post modeling analysis.

### 3.3. UV visible spectroscopy

Shimadzu UV-1700 Spectrophotometer was used to measure UV spectra of free HSA and HSA with varying concentration of MG employing 1 cm path length cell. Initially baseline correction was done using same buffer and the final volume in cuvette was 1 ml.

### 3.4. Intrinsic fluorescence measurement

Shimadzu RF-5301 spectrofluorophotometer was used to record fluorescence spectrum using 10 mm path length quartz cell. The excitation wavelength was set at 280 nm, while the emission spectrum was recorded in the range 300–400 nm.

### 3.5. Advanced Glycation End-Products (AGEs) detection

Fluorescence of maldondialdehyde (MDA)-modified protein and pentosidine (P)-like-fluorescence was monitored by exciting the samples at 370 and 335 nm with emission at 440 and 400 nm, respectively [17]. Concentration of HSA was 50 μM. Solutions were appropriately diluted when necessary.

### 3.6. ANS fluorescence measurements

ANS binding was measured by fluorescence emission with excitation wavelength at 380 nm and emission spectra were recorded from 400 to 600 nm. Protein was incubated with 50 M excess of ANS for 30 min [18].

### 3.7. Thioflavin T (ThT) fluorescence

Modified HSA state was determined as previously described [19]. 100 μl protein solution was mixed with 900 μl ThT reagent (10 μM ThT in 100 mM phosphate, buffer, pH 7.0) and fluorescence was measured at excitation/emission wavelength of 450/482 nm. Fresh HSA solution, dye, and buffer were used as controls.

### 3.8. Congo red (CR) absorbance

Measuring absorbance at 530 nm of amyloid structures in solutions is one of the ways to measure congo red binding to cross-β structure [20]. For this purpose, 2.5 μM albumin-MG and albumin control was incubated in multiples of five with 10 μM congo red in sodium phosphate buffer with 10% (v/v) ethanol. All measurements were made in the
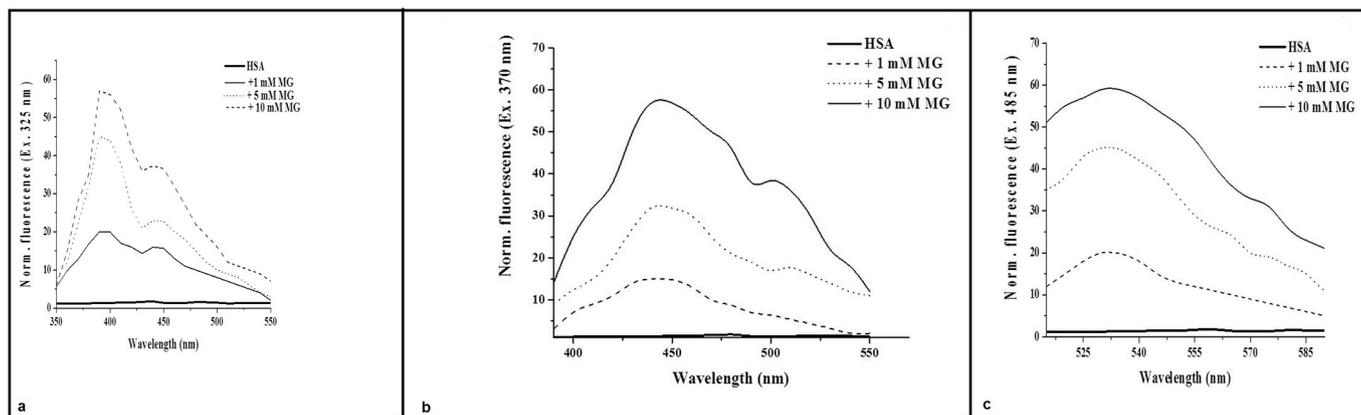


**Fig. 4.** (a) AGEs specific fluorescence of native HSA and HSA incubated with varying MG concentration (1, 5 and 10 mM) modified HSA (excitation: 325 nm; emission: 350–550 nm). (b) AGEs specific fluorescence of native HSA and HSA incubated with varying MG concentration (1, 5 and 10 mM) modified HSA (excitation: 370 nm; emission: 390–550 nm). (c) AGEs specific fluorescence of native HSA and HSA incubated with varying MG concentration (1, 5 and 10 mM) modified HSA ((excitation: 485 nm; emission: 500–550 nm). Spectra were taken at the end of incubation period. All spectra were normalized to the spectrum of the HSA control.
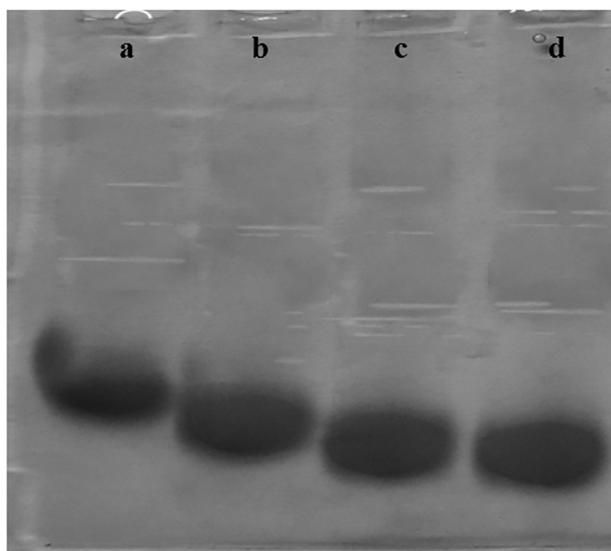
**Fig. 5.** Analysis of MG-HSA by SDS-PAGE. HSA (2 mg/ml) was reacted with 0, 1, 5, 10 mM methylglyoxal in sodium phosphate buffer at 37 °C for 7 days. The lanes from left to right in the PAGE are in ascending order of methylglyoxal concentration used.

range of 220–500 nm in matched quartz cuvettes. Spectra without CR and the one containing CR were compared. Fresh HSA solution, dye, and buffer were used as controls.

### 3.9. Circular dichroism

Circular dichroism spectra of the modified protein and the control, in the far ultraviolet region (190–250 nm) were acquired in a Jasco Spectropolarimeter, model J-720, equipped with a microcomputer, with protein concentrations of about 0.2 g/l and cells having a path length of 0.1 cm [21].

### 3.10. Gel electrophoresis

12.5% SDS-PAGE was performed for samples at different time intervals at 37 °C followed by staining with coomassie brilliant blue according to the method of Laemmli [22].

### 3.11. Scanning electron microscopy

Microscopic analysis was carried out in order to investigate the structure of HSA undergo modification on incubation with methyl glyoxal. Scanning electron microscopy was employed for observing the micro-architecture of the protein. Sample was air dried on cover slip then coated with gold and imaged utilising a JSM-6510LV (JEOL JAPAN) scanning electron microscope.

### 3.12. Transmission electron microscopy

In a bid to have an insight of the morphology of fibrillary structure of HSA, TEM was employed. 10 μl protein sample was placed on a carbon coated copper grid and left to adsorb for 1 min. Further washing of grid was done with distilled water and left to dry. Negative staining with (2%, w/v) aqueous solution of uranyl acetate was done. The excess stain was removed and the samples were allowed to dry. JOEL JEM-2100 (Japan) transmission electron microscope (TEM) operating at 200 kV was done for the analysis of samples.

### 3.13. Replicates

All the experiments were conducted in replicates of four. Each spectrum was recorded as an average of five scans.

## 4. Results and discussion

### 4.1. Modification of HSA by methylglyoxal (MG)

#### 4.1.1. Characterization by fluorescence and UV spectroscopy

*4.1.1.1. UV spectroscopy.* MG induced structural changes in HSA over time were detected by UV spectroscopy (Fig. 1). Fig. 1 depicts the UV absorbance profile of native HSA and HSA incubated with varying concentration of MG for 7 days at room temperature (1, 5 and 10 mM). Native HSA shows a characteristic peak at around 280 nm. For 1 mM MG incubated HSA, increased absorbance was observed with no emergence of a new peak. However, when UV spectra of 5 and 10 mM MG incubated HSA was observed, a strong surge of absorbance was observed over the entire spectrum range. Hiked absorbance at 280 nm is attributed to protein unfolding and exposure of the chromophoric groups [23]. Fig. 1b shows percent increase in absorbance of MG incubated HSA as
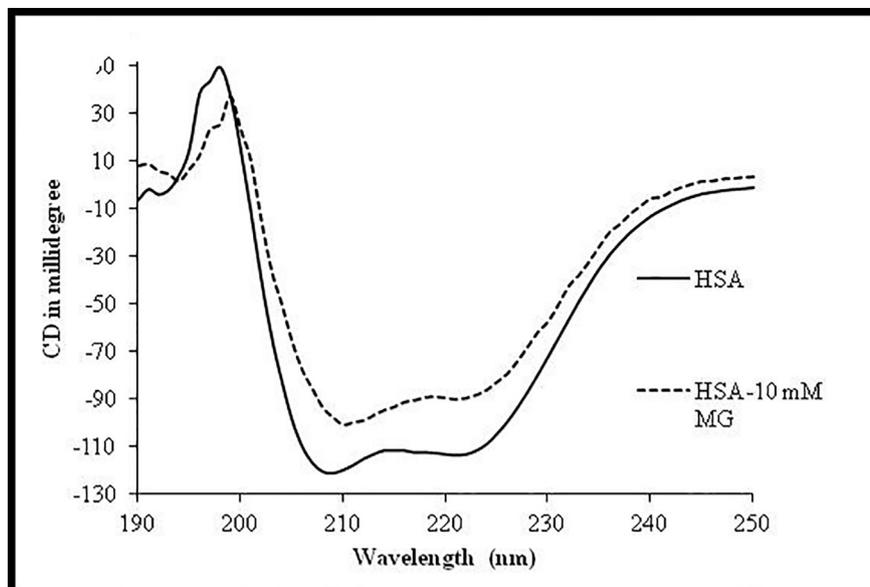


**Fig. 6.** Far UV-CD spectra of native HSA and HSA incubated with 10 mM methylglyoxal. The path length was 0.1 cm and recoding range was 190–250 nm.
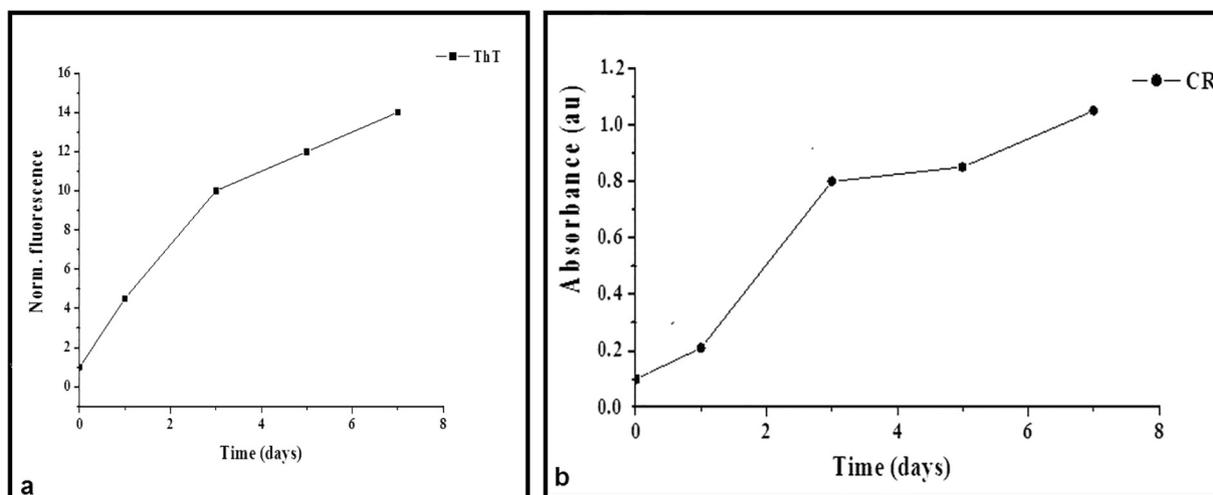
**Fig. 7.** (a) Time dependent changes in the Thioflavin T fluorescence and (b) congo red absorbance of HSA-MG (HSA modified with 10 mM MG). For ThT fluorescence, excitation wavelength used was 450 nm and recording range was 455–600 nm. For congo red binding, the absorbance at 530 nm was recorded.

compared to native HSA as a function of time; maximum increase occurring after 7 days. A characteristic new peak could be seen at around 320–330 nm for 5 and 10 mM MG incubated HSA. The increased absorbance and emergence of new peaks quite clearly suggests that MG has induced a structural alteration in native structure of HSA thereby modifying it to non-native form; 10 mM MG being the most effective.

*4.1.1.2. Intrinsic fluorescence.* The changes in native conformation of HSA by MG as found out by UV spectroscopy were further explored by making use of intrinsic fluorescence. Intrinsic fluorescence is an interesting tool to follow AGE's formation. The intrinsic fluorescence spectra (Fig. 2a) correspond with UV spectral profile and confirm that MG induces structural transition of native HSA towards non-native form. As is evident in Fig. 2a, intrinsic fluorescence of HSA decreased with increasing MG concentration. At 1 mM MG, only a small decrease (~12%) could be observed while in the presence of 5 mM glyoxal this decrease was ~50% reaching to a maximum of 85% decline at 10 mM MG. Changes in fluorescence intensity with time re depicted in Fig. 2b. The decrease in fluorescence intensity was also time dependent with maximum decrease occurring on the seventh day of incubation. Further incubation had no effect fluorescence intensity. Thus, it is quite evident that intrinsic fluorescence decreases in a concentration dependent as well as time dependent manner. Interestingly, an increase in the fluorescence is also observed at 395 nm and 440 nm till 5 mM MG concentration. These

two additional peaks may be due to glycation induced glycophoric moieties. However, at 10 mM MG, no such increase was noticeable. A decrease in intrinsic protein fluorescence caused by tryptophan was previously reported by Coussons et al. [1997] for glycated HSA [5]. A robust decrease in intrinsic fluorescence was recorded in their experiments with increasing sugar concentrations. On the contrary, no detection in modification of tryptophan was there even after 56 days of incubation with 0.5 M sugar concentration. Therefore, it is quite clear that decrease in intrinsic fluorescence of HSA in the presence of MG can be owed to conformational change in HSA induced by MG.

*4.1.1.3. ANS fluorescence.* ANS is a widely utilized fluorescent probe for the characterization of protein binding sites. A weak fluorescence is emitted in polar environment while fluorescence emission drastically increases when bound to hydrophobic patches on proteins coupled with an observed hypsochromic shift. A blue shift of fluorescence emission maxima is an evident feature of ANS and is generally owed to the hydrophobicity of the binding site [24]. To evaluate the alterations in the HSA conformation in presence of MG, ANS binding to the modified HSA was measured (Fig. 3). A considerable increase in ANS fluorescence coupled with a blue shift of ₋20 nm was observed for 10 mM MG incubated HSA. This is indicative of the solvent exposure of hydrophobic patches of the protein. Thus, it is quite evident from this assay that
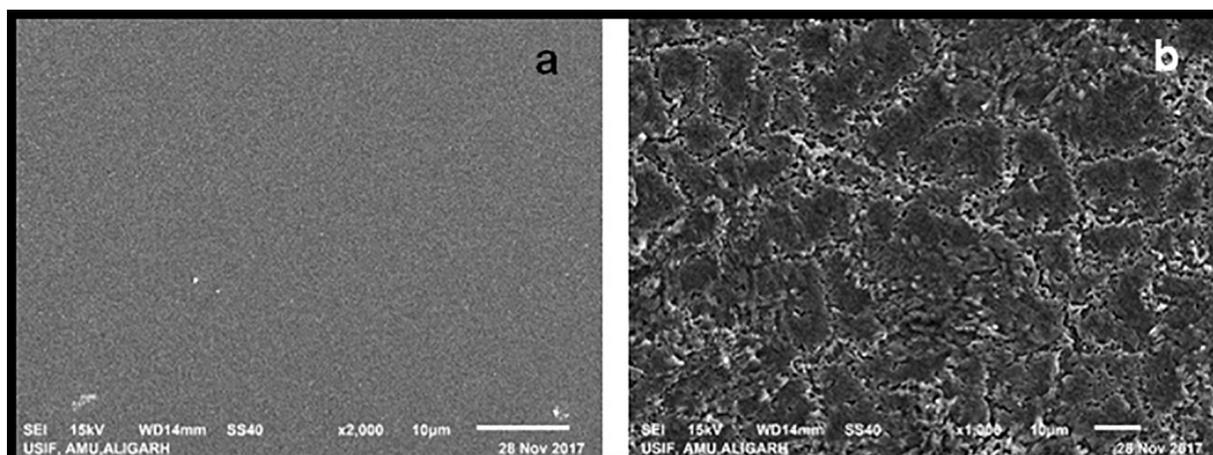


**Fig. 8.** SEM analysis of (a) native HSA and (b) HSA incubated with 10 mM methylglyoxal.
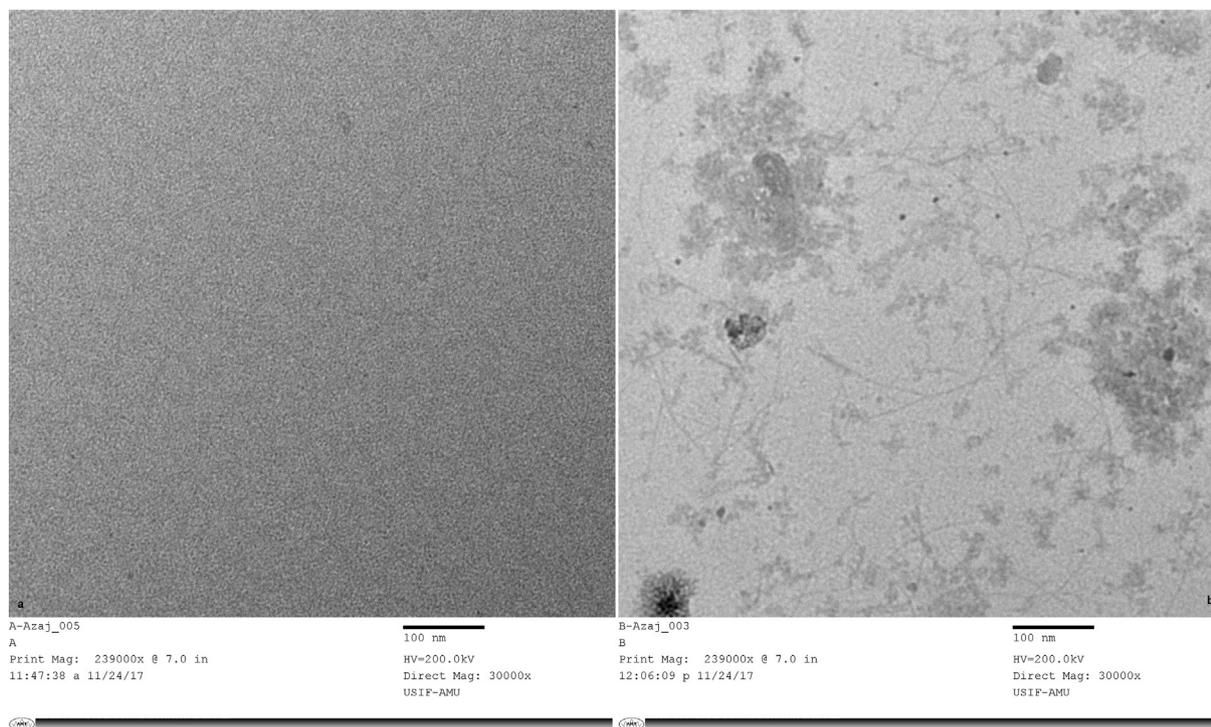
**Fig. 9.** TEM analysis of (a) native HSA and (b) 10 mM MG incubated HSA.

MG induces structural transition of HSA; 10 mM MG causing the maximum structural alterations.

### 4.1.2. Advanced glycation end-products (AGEs) detection

Incubation of biomolecules with sugars or sugar degradation products results in the formation of glycophores or advanced glycation end products (AGEs). The fluorophores that are formed as a result of reaction of sugars with lysine, arginine etc. are also called as AGEs. There is a characteristic fluorescence emission maxima exhibited by these viz. pentosidine, argpyrimidine shows glycation specific fluorescence that can be employed for detection of AGEs [25]. Fig. 4 shows the AGE formation over incubation time as studied by non-tryptophan fluorescence spectroscopy. Formation of three different AGEs upon incubation of HSA with MG was analyzed using the excitation wavelengths of 325, 370 and 485 nm as described by Schmitt et al. 2005 [26]. A high absorbance between 320 nm and 335 nm is observed for argpyrimidine. Pentosidine also absorbs between 325 and 335 nm. For excitation at

325 nm, emission at 395 nm has been reported [27] for glucose modified HSA. This fluorescence accounts for argpyrimidine and pentosidine, both well-known AGE structures derived from arginine [28]. For emission at 440 nm, the excitation maximum has been reported to be 370 nm. The fluorescence at excitation/emission wavelength of 370/440 nm has been reported for AGE-modified lens proteins by Monnier and Cerami 1981 [29] and was found to be a useful tool to determine the total AGE fluorescence [30]. This excitation wavelength at 370 nm is definite for malondialdehyde-modified protein-like fluorescence. Fig. 4a shows the fluorescence spectra recorded at an excitation wavelength of 325 nm. For all concentrations of MG (1, 5 and 10 mM), an increased fluorescence could be observed at emission wavelengths of 395 and 440 nm; maximum fluorescence observed for 10 mM MG incubated HSA. However, the fluorescence with emission at 440 nm remained almost constant. For excitation at 370 nm, an emission peak was obtained at 440 nm. The fluorescence intensity increased in a concentration dependent manner (Fig. 4b); maximum increase observed for 10 mM MG. Upon excitation at 485 nm, the maximum emission was detected at around 530 nm. The intensity at 530 nm increased gradually with increase in MG concentration (Fig. 4c); maximum fluorescence observed for 10 mM MG implying maximum AGEs formation at this concentration. Thus from these AGEs specific fluorescence assay, it can be concluded that 10 mM MG over the span of 7 days induces the formation of AGEs of HSA in way distorting the native structure of HSA.

### 4.1.3. Characterization by PAGE

SDS-PAGE of the MG incubated HSA demonstrated that the electrophoretic mobility of HSA increases with increase in MG concentration (Fig. 5). This clearly indicates that there is a progressive loss of positive charge in the MG-HSA during glycation reaction; maximum observed for 10 mM MG incubated HSA.

### 4.1.4. Secondary structural analysis by CD

The secondary structural changes induced in HSA by MG were assessed making use of CD spectroscopy as CD spectra are responsive to changes in secondary structure of proteins. For alpha helix rich proteins, CD spectra show two negative peaks, one at 208 nm and second
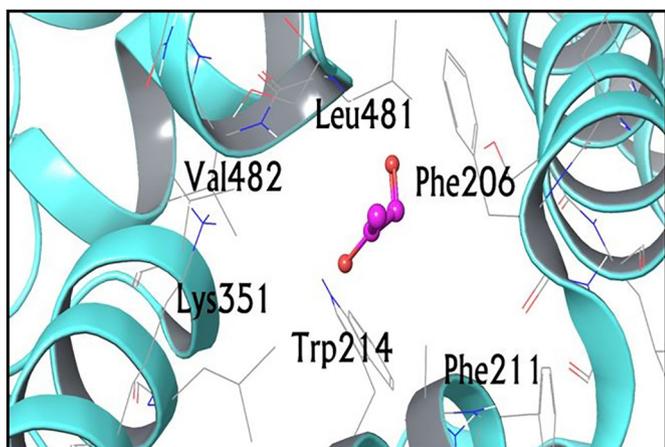


**Fig. 10.** Docking studies. Methylglyoxal molecule in the vicinity of HSA and trapped in the interior showing various residues involved in this interaction.

at 222 nm; while proteins having beta sheets show a negative peak at around 218 nm. Fig. 6 shows the far UV-CD spectra of native HSA and from the figure it is quite evident that two negative peaks are observed at around 208 nm and 222 nm. These negative peaks are characteristic of α-helix conformation [31]. When there is an upward shift in spectrum, it indicates that there is a reduction in helical structure while increased helical structure is related to a downward shift in the spectrum. No significant changes were observed in the far UV-CD spectrum of the HSA-MG for 1 and 5 mM MG concentration (data not shown). However, at 10 mM MG, an appreciable decline in the α-helical was observed (21% decline from the native) and this decrease in α-helical content can be owed to the fact that there is an increase in the unordered structure in the presence of 10 mM MG. These evident changes in secondary structure of HSA in the presence of MG strongly supports the MG induced AGEs formation of HSA as secondary structural changes for other proteins upon glycation are well documented in literature [32].

### 4.1.5. Aggregation study

#### 4.1.5.1. Thioflavin T (ThT) fluorescence.
ThT is often employed dye in a bid to detect the fibrillar state of protein. It is well reported for several proteins that glycation leads to aggregation [10]. Thus it is evident that glycation of polypeptides, which have the propensity to condensate into amyloid fibrils, can accelerate cross β structure formation. Thus, analysis of the ThT fluorescence of the HSA-MG was undertaken (Fig. 7a). No appreciable changes in ThT fluorescence was detected at 1 mM MG concentration. An increase in ThT fluorescence (evidently time-dependent) was observed at 10 mM MG. Increase in ThT fluorescence suggests that glycation with MG induce HSA to aggregates formation, when left for a prolonged time period [33].

#### 4.1.5.2. Congo red absorbance.
CR is a symmetrical sulfonated azo dye which consists of a hydrophobic centre with biphenyl group spaced between the negatively charged sulfate groups. To further confirm the ThT results, CR assay was also employed. The results obtained for CR assay were consistent with ThT assay results. It is quite evident that a time dependent increase in CR absorbance was observed for 10 mM MG incubated HSA (Fig. 7b); maximum absorbance recorded at 7th day. The results obtained for ThT and CR are consistent.

#### 4.1.5.3. Scanning electron microscopy.
Scanning electron microscopy was performed with a view to have an insight into the traits of species that are formed when HSA in incubated with 10 mM MG for 7 days. Fig. 8a shows the SEM analysis of native HSA while Fig. 8b represents the SEM analysis of 10 mM MG incubated HSA. As is quite evident from Fig. 8b, 10 mM MG induces the formation of aggregates of HSA which are clearly visible. Thus, it is quite evident that glycation of HSA results in the formation of aggregates of HSA.

#### 4.1.5.4. Transmission electron microscopy (TEM).
From Fig. 9 it is quite evident that 10 mM MG induces formation of HSA aggregates which are clearly visible in the TEM analysis. No aggregated structure of the protein is observed for HSA and protein is in its native state (Fig. 9a) while clear aggregates (fibrillar type) are observed for 10 mM MG incubated HSA (Fig. 9b).

### 4.1.6. Molecular docking study

Molecular docking analysis gives an insight [34] of the important residues that play a part in MG-HSA interaction. Fig. 10 depicts the residues that are involved in this site specific interaction viz. HSA is depicted in the ribbon form while methylglyoxal is shown in the form of sticks. Different residues that are involved in this reaction are Lys 351, Leu 481, Val 482, Trp 214 and Phe 206, 211. The detected binding site of methylglyoxal to HSA is of significance as it can serve a very important role in the field of drug designing as HSA is a clinically relevant protein playing crucial role in many diseases.

## 5. Conclusion

In our present study, the model protein that has been used is HSA while MG has been used as an organic solvent to mimic in vitro conditions for studying the glycation and aggregation pattern of HSA. It is found that in the presence of MG, HSA is modified to a non-native form as evident by changes in UV spectra and intrinsic fluorescence spectra of MG incubated HSA; maximum changes observed for 10 mM MG incubated HSA suggesting this concentration to be maximally effective. Furthermore, changes in CD spectra clearly suggests changes in secondary structure of HSA in the presence of 10 mM MG. AGEs specific fluorescence clearly suggests formation of AGEs of HSA when incubated with MG for a span of 7 days; maximum AGEs formation occurring for 10 mM MG incubated HSA. Microscopy were further provided an insight into the nature of aggregates of HSA in the presence of 10 mM MG. Specific residues involved in the MG-HSA interaction were revealed making use of molecular docking which can further serve as an asset in the field of drug designing owing to clinical significance of both MG and HSA.

## References

[1] M.M. Anderson, J.R. Requena, J.R. Crowley, S.R. Thorpe, J.W. Heinecke, The myeloperoxidase system of human phagocytes generates Nε-(carboxymethyl) lysine on proteins: a mechanism for producing advanced glycation end products at sites of inflammation, J. Clin. Invest. 104 (1999) 103.

[2] D.C. Carter, J.X. Ho, Structure of serum albumin, Adv. Protein Chem. 45 (1994) 153–203.

[3] N. Ahmed, P.J. Thornalley, Peptide mapping of human serum albumin modified minimally by methylglyoxal in vitro and in vivo, Ann. N. Y. Acad. Sci. 1043 (2005) 260–266.

[4] T. Peters Jr., All About Albumin: Biochemistry, Genetics, and Medical Applications, Academic press, 1995.

[5] P.J. Coussons, J. Jacoby, A. McKay, S.M. Kelly, N.C. Price, J.V. Hunt, Glucose modification of human serum albumin: a structural study, Free Radic. Biol. Med. 22 (1997) 1217–1227.

[6] S. Amani, A. Shamsi, G. Rabbani, A. Naim, An insight into the biophysical characterization of insoluble collagen aggregates: implication for arthritis, J. Fluoresc. 24 (2014) 1423–1431, https://doi.org/10.1007/s10895-014-1424-x.

[7] S. Amani, A. Naeem, Detection and analysis of amorphous aggregates and fibrils of cytochrome c in the presence of phenolic acids, Int. J. Biol. Macromol. 58 (2013) 104–112, https://doi.org/10.1016/j.ijbiomac.2013.03.055.

[8] T.T. Herskovits, H. Jaillet, Structural stability and solvent denaturation of myoglobin, Science 163 (1969) 282–285.

[9] R. Singh, A. Barden, T. Mori, L. Beilin, Advanced glycation end-products: a review, Diabetologia 44 (2001) 129–146.

[10] A. Shamsi, A. Ahmed, B. Bano, Glyoxal induced structural transition of buffalo kidney cystatin to molten globule and aggregates: anti-fibrillation potency of quinic acid, IUBMB Life 68 (2016) 156–166.

[11] P. Alam, S.K. Chaturvedi, M.K. Siddiqi, R.K. Rajpoot, M.R. Ajmal, M. Zaman, R.H. Khan, Vitamin k3 inhibits protein aggregation: implication in the treatment of amyloid diseases, Sci. Rep. 6 (2016) 26759.

[12] M.K. Siddiqi, P. Alam, S.K. Chaturvedi, S. Nusrat, Y.E. Shahein, R.H. Khan, Attenuation of amyloid fibrillation in presence of warfarin: a biophysical investigation, Int. J. Biol. Macromol. 95 (2017) 713–718.

[13] P. Alam, A.Z. Beg, M.K. Siddiqi, S.K. Chaturvedi, R.K. Rajpoot, M.R. Ajmal, M. Zaman, A.S. Abdelhameed, R.H. Khan, Ascorbic acid inhibits human insulin aggregation and protects against amyloid induced cytotoxicity, Arch. Biochem. Biophys. 621 (2017) 54–62.

[14] N.A. Al-Shabib, J.M. Khan, M.A. Alsenaidy, A.M. Alsenaidy, M.S. Khan, F.M. Husain, M.R. Khan, M. Naseem, P. Sen, P. Alam, R.H. Khan, Unveiling the stimulatory effects of tartrazine on human and bovine serum albumin fibrillogenesis: spectroscopic and microscopic study, Spectrochim. Acta A Mol. Biomol. Spectrosc. 191 (2018) 116–124.

[15] O.H. Lowry, N.J. Rosebrough, A.L. Farr, R.J. Randall, Protein measurement with the Folin phenol reagent, J. Biol. Chem. 193 (1951) 265–275.

[16] O. Trott, A.J. Olson, AutoDock Vina: improving the speed and accuracy of docking with a new scoring function, efficient optimization, and multithreading, J. Comput. Chem. 31 (2010) 455–461.

[17] A. Naeem, T.A. Khan, M. Muzaffar, S. Ahmad, M. Saleemuddin, A partially folded state of ovalbumin at low pH tends to aggregate, Cell Biochem. Biophys. 59 (2011) 29–38.

[18] A. Naeem, S. Amani, Deciphering structural intermediates and genotoxic fibrillar aggregates of albumins: a molecular mechanism underlying for degenerative diseases, PLoS One 8 (2013), e54061. .

[19] M. Priyadarshini, B. Bano, Conformational changes during amyloid fibril formation of pancreatic thiol proteinase inhibitor: effect of copper and zinc, Mol. Biol. Rep. 39 (2012) 2945–2955.

[20] B. Bouma, L.M. Kroon-Batenburg, Y.-P. Wu, B. Brünjes, G. Posthuma, O. Kranenburg, P.G. de Groot, E.E. Voest, M.F. Gebbink, Glycation induces formation of amyloid cross-$\beta$ structure in albumin, J. Biol. Chem. 278 (2003) 41810–41819.

[21] M.R. Ajmal, A.S. Abdelhameed, P. Alam, R.H. Khan, Interaction of new kinase inhibitors cabozantinib and tofacitinib with human serum alpha-1 acid glycoprotein. A comprehensive spectroscopic and molecular docking approach, Spectrochim. Acta A Mol. Biomol. Spectrosc. 159 (2016) 199–208.

[22] U.K. Laemmli, Cleavage of structural proteins during the assembly of the head of bacteriophage T4, Nature 227 (1970) 680–685.

[23] N. Traverso, S. Menini, D. Cottalasso, P. Odetti, U.M. Marinari, M.A. Pronzato, Mutual interaction between glycation and oxidation during non-enzymatic protein modification, Biochim. Biophys. Acta BBA-Gen. Subj. 1336 (1997) 409–418.

[24] S. Amani, A. Naeem, Deciphering aggregates, prefibrillar oligomers and protofibrils of cytochrome c, Amino Acids 46 (2014) 1839–1851, https://doi.org/10.1007/s00726-014-1698-y.

[25] S.W. Vetter, V.S. Indurthi, Moderate glycation of serum albumin affects folding, stability, and ligand binding, Clin. Chim. Acta 412 (2011) 2105–2116.

[26] A. Schmitt, J. Schmitt, G. Münch, J. Gasic-Milencovic, Characterization of advanced glycation end products for biochemical studies: side chain modifications and fluorescence characteristics, Anal. Biochem. 338 (2005) 201–215, https://doi.org/10.1016/j.ab.2004.12.003.

[27] M.E. Westwood, P.J. Thornalley, Molecular characteristics of methylglyoxal-modified bovine and human serum albumins. Comparison with glucose-derived advanced glycation endproduct-modified serum albumins, J. Protein Chem. 14 (1995) 359–372.

[28] N. Ahmed, D. Dobler, M. Dean, P.J. Thornalley, Peptide mapping identifies hotspot site of modification in human serum albumin by methylglyoxal involved in ligand binding and esterase activity, J. Biol. Chem. 280 (2005) 5724–5732.

[29] V.M. Monnier, A. Cerami, Detection of nonenzymatic browning products in the human lens, Biochim. Biophys. Acta BBA-Gen. Subj. 760 (1983) 97–103.

[30] S.D. Sharma, B.N. Pandey, K.P. Mishra, S. Sivakami, Amadori product and age formation during nonenzymatic glycosylation of bovine serum albumin in vitro, J Biochem Mol Biol Biophys. 6 (2002) 233–242.

[31] G.R. Upchurch, N. Ramdev, M.T. Walsh, J. Loscalzo, Prothrombotic consequences of the oxidation of fibrinogen and their inhibition by aspirin, J. Thromb. Thrombolysis 5 (1998) 9–14.

[32] U. Dutta, M.A. Cohenford, J.A. Dain, Monitoring the effect of glucosamine and glyceraldehyde glycation on the secondary structure of human serum albumin and immunoglobulin G: an analysis based on circular dichroism, thermal melting profiles and UV–fluorescence spectroscopy, Anal. Chim. Acta 558 (2006) 187–194.

[33] Y. Wei, L. Chen, J. Chen, L. Ge, R.Q. He, Rapid glycation with D-ribose induces globular amyloid-like aggregations of BSA with high cytotoxicity to SH-SY5Y cells, BMC Cell Biol. 10 (2009) 10.

[34] S. Khatun, Riyazuddeen, Interaction of colchicine with BSA: spectroscopic, calorimetric and molecular modeling approaches, J. Biomol. Struct. Dyn. (2017) 1–8.